AFRL-AFOSR-JP-TR-2020-0008

Ionosphere irregularities in South Pacific

Sushil Kumar
University of South Pacific
LAUCALA BAY ROAD
SUVA, PMB
FJ

07/27/2020
Final Report

Air Force Research Laboratory
Air Force Office of Scientific Research
Asian Office of Aerospace Research and Development
Unit 45002, APO AP 96338-5002

REPORT DOCUMENTATION PAGE

Form Approved
OMB No. 0704-0188

1. REPORT DATE *(DD-MM-YYYY)*	2. REPORT TYPE	3. DATES COVERED *(From - To)*
27-07-2020	Final	19 Apr 2017 to 18 Jan 2021

4. TITLE AND SUBTITLE
Ionosphere irregularities in South Pacific

5a. CONTRACT NUMBER

5b. GRANT NUMBER
FA2386-17-1-0054

5c. PROGRAM ELEMENT NUMBER
61102F

6. AUTHOR(S)
Sushil Kumar

5d. PROJECT NUMBER

5e. TASK NUMBER

5f. WORK UNIT NUMBER

7. PERFORMING ORGANIZATION NAME(S) AND ADDRESS(ES)
University of South Pacific
LAUCALA BAY ROAD
SUVA, PMB FJ

8. PERFORMING ORGANIZATION REPORT NUMBER

9. SPONSORING/MONITORING AGENCY NAME(S) AND ADDRESS(ES)
AOARD
UNIT 45002
APO AP 96338-5002

10. SPONSOR/MONITOR'S ACRONYM(S)
AFRL/AFOSR IOA

11. SPONSOR/MONITOR'S REPORT NUMBER(S)
AFRL-AFOSR-JP-TR-2020-0008

12. DISTRIBUTION/AVAILABILITY STATEMENT
A DISTRIBUTION UNLIMITED: PB Public Release

13. SUPPLEMENTARY NOTES

14. ABSTRACT
The South Pacific region covers belt of equatorial and low latitudes hence offers unique locations for experimenting and studying the characteristic variations in total electron content (TEC) and L- band scintillation. Understanding of this connection is of utmost importance for existing and future planning of satellite communication links. The main goal of the project was to investigate space weather effects on the ionospheric electron content and GPS L band scintillation at equatorial (Kiribati) to low latitude (Suva, Fiji) in the South Pacific Region which has not been explored in-depth so far. A Global Navigation Satellite System (GNSS) receiver was installed at the University of the South Pacific campus in Tarawa to study the TEC and L-band scintillations. The geomagnetic storms at Tamara station were observed between September 2017 and November 2018. The data was subsequently analyzed to determine relationship between storm phase TEC and L-band scintillation.

15. SUBJECT TERMS
ionosphere, GPS scintillation, AOARD

16. SECURITY CLASSIFICATION OF:			17. LIMITATION OF ABSTRACT	18. NUMBER OF PAGES	19a. NAME OF RESPONSIBLE PERSON
a. REPORT	b. ABSTRACT	c. THIS PAGE			KIM, TONY
Unclassified	Unclassified	Unclassified	SAR		19b. TELEPHONE NUMBER *(Include area code)* 315-227-7008

Standard Form 298 (Rev. 8/98)
Prescribed by ANSI Std. Z39.18

Final Report for AOARD Grant FA2386-17-1-0054

Ionosphere irregularities in South Pacific

Project Title: Space Weather effects on Ionospheric electron content and L band scintillation at Equatorial and Low latitudes

Date: 16 July 2020

Name of Principal Investigators (PI and Co-PIs):

- e-mail address : kumar_su@usp.ac.fj
- Institution : The university of the South Pacific, Fiji.
- Mailing Address : Private Mail Bag, Laucala Bay Road, Suva, Fiji
- Phone : +679-3232144
- Fax : +679-3231416

Period of Performance: Month/Day/Year – Month/Day/Year
19 January 2017 to 18 January 2020

Abstract: Short summary of most important research results that explain why the work was done, what was accomplished, and how it pushed scientific frontiers or advanced the field. This summary will be used for archival purposes and will be added to a searchable DoD database.

The changes in the critical frequency of F2-layer (f_oF_2) and f_oF_2 deviation (Δf_oF_2) from monthly median level were determined for three geomagnetic storms in March of the years 2012, 2013, and 2015 at low latitude stations, Darwin (geomag. lat. 21.96°S) and Townsville (28.95°S), and mid-latitude stations, Brisbane (36.73°S), Canberra (45.65°S) and Hobart (54.17°S). St. Patrick day geomagnetic storm of 17-19 March 2015 was the most intense storm of the current solar cycle 24 with a minimum of Dst index reaching -222 nT. This storm is the most studied space weather events of solar cycle 24, and our results contributed to a knowledge gap that was existing from the southern hemisphere region.

The initial results of TEC data for one year (September 2017 to August 2018), which falls under a low solar activity period with average sunspot number 11.6, have been analyzed at an equatorial station, Tarawa, Kiribati (geog.1.45° N, 172.97° E, geomag. 2.45°S, 114.00°W). Seasonally, equinox showed maximum VTEC, summer showed plateau effects while winter showed TEC bite-outs. Scintillations both on L1 and L2 band signals occuured only in the nighttime which started developing around 20:00 LT reaching a peak around 23:00 LT and denisnished before 03:00 LT. In addition to the above, the effect of the geomagnetic disturbance showed higher VTEC on magnetically disturbed days as compared to quiet days.

The effects of a complex severe space weather event of 4-9 September 2017 on vertical total electron content (VTEC) and L1 and L2 band ionospheric scintillations were analyzed. The previous studies on effects of 4-17 September 2017 space weather events concentrated mainly on strong solar flares of X class on 06 September and GPS L1 band scintillations. In the present work, we have analyzed the equatorial

vertical TEC (VTEC) response to the strong M class solar flares that occurred on 4-5 September under geomagnetically quiet conditions. In particular, equatorial ionospheric response to M5.5 and M4.2 class flares that occurred during the sunlit at an equatorial station, Tarawa, were analyzed. The VTEC increased significantly by 1.03 and 1.31 TEC units under M5.5 flare at 20:28 UT on 04 September and M4.2 flare at 01:03 UT on 05 September, respectively, under the quiet geomagnetic conditions. A positive ionospheric storm with a maximum percentage change in VTEC (ΔVTEC%) of 16.7% followed by a negative ionospheric storm with ΔVTEC% of 32.8% occurred during the first main phase (*Dst* = - 142 nT) and recovery of 7-8 September storm.

To study the effect of the geomagnetic storms on VTEC and scintillation, a total of seven geomagnetic storms of moderate (*Dst* index= -55nT) to intense (*Dst* index= -174nT) category that occurred during the period from September 2017 to November 2018, were analyzed. The results showed both positive and negative ionospheric storm effects in VTEC during the main and recovery phases of the storms. The positive ionospheric storms were dominant in all the local time sectors and were generally confined near the main phase of the geomagnetic storm whereas the negative storms were rare and occurred only after local sunset hours. The VTEC, amplitude, and phase scintillation index measured from all GPS satellite signals observed previously at Suva, Fiji, were also analyzed for geomagnetic storms of 1 – 4 March 2011 (moderate), 6 – 10 March 2012 (intense), 15 - 17 March 2012 (Intense), 13 – 17 July 2012 (intense), 6- 10 Oct 2012 (moderate), 13 – 15 October 2012 (moderate) to compare with the storm analysis at Tarawa station.

Introduction: Include a summary of specific aims of the research and describe the importance and ultimate goal of the work.

The South Pacific region covers belt of equatorial and low latitudes hence offer s unique locations for experimenting with studying the characteristic variations i n TEC and L band scintillation which is of utmost importance for existing and future planning of satellite communication links. It also provides a great opportu nity to investigate the long term effects of the variations in the ionospheric TEC a nd scintillations due to solar and geomagnetic activities that have not been investig ated in-depth for this region. This main goal of the project was to investigate sp ace weather effects on the ionospheric electron content and GPS L band scintill ation at equatorial (Kiribati) to low latitude (Suva, Fiji) in the South Pacific Re gion that has not been explored in-depth so far. The following specific aims we re proposed to achieve the aim of the project.

1. Analyse diurnal and seasonal variations of TEC and L_1 band scintillations during current solar cycle.
2. Investigate geomagnetic storm and solar flare effects on TEC and scintillation.
3. Analyse latitudinal variation of TEC and scintillation activity by analysing the data at equatorial and low latitude stations under space weather conditions.

4. Determine FFT and Wavelet spectra for L_1 band scintillations to study spectral properties and the dynamics of ionospheric irregularities causing GPS scintillations.

Experiment: Description of the experiment(s)/theory and equipment or analyses.

A Global Navigation Satellite System (GNSS) receiver was installed at The University of the South Pacific campus in Tarawa (geographic coordinates: 1.33ºN, 173.01ºE, geomagnetic coordinates: 2.68ºS, 114.26º W), Kiribati, on 4 September 2017, to study the TEC and L band scintillations. The setup consists of a Septentrio PolaRx5S receiver, PolaNt Choke Ring B3/E6 antenna mounted at the roof of the station, and connected to the PolaRx5S receiver along with other necessary hardware and data recording software.

Septentrio PolaRx5S receiver is a multi-frequency, multi-constellation receiver designed for space weather monitoring and applications. The receiver works with a user graphical interface (UGI) logging tool (Rx Tools) for continuous monitoring and recording of the data. It is capable of recording of L1, L2, and L5 signals and uses them to give some of the most important ionospheric parameters such as TEC, changes in TEC (dTEC), amplitude and phase scintillation indices (S_4, σ_Φ) and scintillation index (*SI*). The receiver also allows real-time output on all GNSS L-band signals and can provide a common output file for the data (*Septentrio*, 2016). Septentrio PolaNt Choke Ring B3/E6 antenna- is an aluminum-based high precision geodetic multi-frequency, multi-constellation choke ring antenna which supports full range of GNSS signals. The major advantage of using this antenna is that its choke ring characteristic provides low phase-center variation and better multi-path rejection which with the inclusion of low-noise amplifiers provides an accurate and reliable data recording.

The TEC given by the receiver system is based on dual-frequency pseudorange measurements while the dTEC is based on carrier phase measurements (*Septentrio*, 2016). The receiver outputs absolute TEC values every 15 seconds giving the TEC average at times, 15, 30, 45, and 60 sec and as such we have used one minute averaged TEC for the absolute/slant TEC (STEC).

For the receiver to give TEC in an acceptable range, it needed to be calibrated. The receiver records and compares at least a 24-hour sample data with the Klobacher Ionospheric Model and applies any calibration which is needed. The calibration also includes any differential code bias to correct for TEC biases. Regarding the recording station's location, our TEC data recorded was calibrated with 17.47 TECU which the receiver corrects automatically once the daily data are recorded. The receiver corrects the STEC values using the equation:

$$STEC = STEC_{initial} - 17.47 \quad (1)$$

The receiver records and outputs the amplitude scintillation index S_4 on L1, L2 and L5 band signals. The S_4 is recorded by the receiver as the SD (σ) of 50 Hz raw signal

power normalized to the average signal power over one minute (S_{4total}). The receiver also outputs the correction due to thermal noise as S_{4cor} and the final S_4 is given by:

$$S_4 = \sqrt{S_{4_{total}} - S_{4_{cor}}} \qquad (2)$$

If $S_{4cor} > S_{4total}$, then S_4 is taken as zero. Similar to S_4, the receiver also records and outputs phase scintillation (σ_Φ) on L band signals (L1, L2, and L5). The σ_Φ is recorded as the σ sampled at 50 Hz by detrending the carrier phase averaged over the interval of 1, 3, 10, 30 and 60 seconds on each band signal and we have used 1-minute interval values. Also, the receiver detrends the raw carrier phase measurements using a 6th Butterworth high pass filter.

Scintillation index (SI) in dB is computed as follows:

$$SI(dB) = 10\,[\log_{10} P_{max} - \log_{10} P_{min}] \qquad (3)$$

Where P_{max} is conventionally defined as the power amplitude of the third peak down from the maximum excursion over the 3000 samples at the last minute, and P_{min} is the power amplitude of the third level up from the minimum excursion.

The data recorded by the receiver were analyzed using Matlab. A live script was written in Matlab which removed all the data entry having signal lock time less than 240 seconds and elevation angle less than 50° so that the ionospheric pierce point (IPP) could be used as a constant of 350 km for the station during the calculation of TEC and to avoid any data with multipath effects (Prasad et al., 2016).

The slant TEC (STEC) from the receiver was converted to vertical VTEC using the Thin Shell Model outlined and used by several researchers (e.g., Afraimovich *et al*., 2002; Klobuchar, *1987*; Nava *et al*., 2007; Prasad *et al*., 2016):

$$VTEC = STEC \times \left[1 - \left(\frac{R_E Cos\theta}{R_E + h_{IPP}}\right)^2\right]^{1/2} \qquad (4)$$

Where R_e = mean radius of earth- 6378.14 km, h_{IPP} = ionospheric pierce point, 350 km, θ = satellite elevation angle. We also calculated the percentage changes in VTEC (ΔVTEC %) during the storm time from the mean VTEC on the five geomagnetically quiet days using:

$$\Delta VTEC\ \% = \frac{VTEC_{storm} - VTEC_{quiet}}{VTEC_{quiet}} \times 100 \qquad (5)$$

The diurnal minima in VTEC occurred at around 05 LT and maxima around 14 LT. The scintillations, both on L1 and L2 bands occurred mainly during the pre-midnight period (18-06 LT) with larger occurrence on L2 band signal than on L1 band signal and strong scintillation ($S_4 > 0.45$) occurred only on L2 band signal.

Results and Discussion: Describe significant experimental and/or theoretical research advances or findings and their significance to the field and what work may be performed in the future as a follow on project. Fellow researchers will be interested

to know what impact this research has on your particular field of science.

A typical variation in VTEC (TEC units, 1TECU = 10^{17}elm^{-3}) on 4th January 2018 at Tarawa, Kiribati (geog. lat. 1.45° N, long. 172.97° E, geomag. lat. 2.45°S, long. 114.00°W) shown in Figure 1. The diurnal maxima in VTEC occurred between 14:00-15:00 LT. The minimum in VTEC occurred at around 06 LT and maxima around 15 LT. The VETC was then calculated on monthly basis for 12 months (December 2017 to November 2018) from which seasonal VTEC was calculated and shown in Figure 2. The VTEC was maximum during equinox followed by winter and summer. The seasonal analysis revealed that the equinox had two maximum VTEC peaks with the highest VTEC due to the orientation of the earth's plane relative to the sun. This orientation also causes an increase in the O/N_2 gas ratio which has also been stated as one of the reasons for high VTEC in the equinox season. The analysis also revealed seasonal dependence, winter anomaly, TEC bite-outs, and semi-annual cycle in the VTEC data.

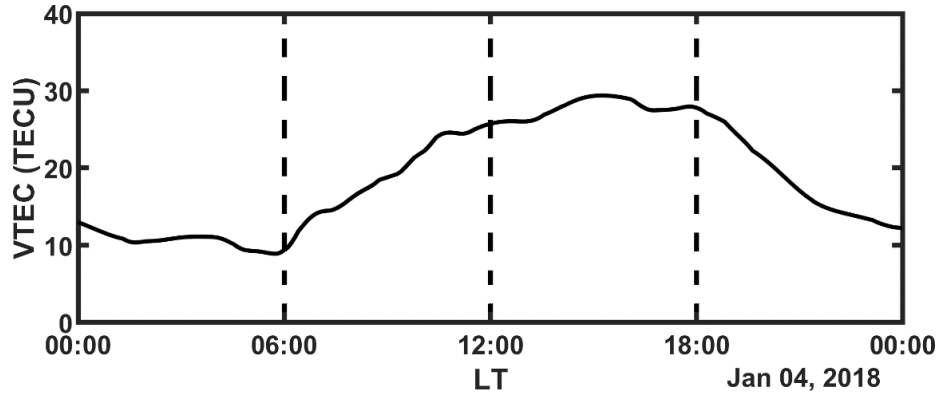

Figure 1: Diurnal variation of VTEC at Tarawa on a geomagnetic quiet day (January 4th, 2018).

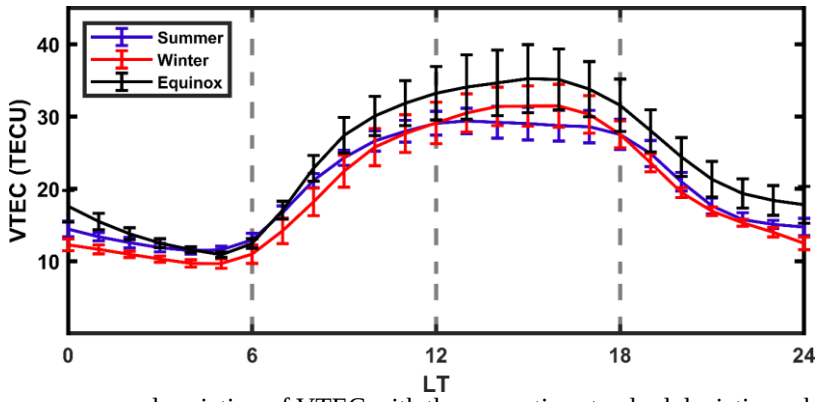

Figure 2: Average seasonal variation of VTEC with the respective standard deviations shown as error bars.

The occurrence of scintillation at Tarawa was measured by the S_4 index on L_1 and L_2 band signals of GPS constellation. The scintillation events were categorized as very weak, weak, moderate and strong events based on the S_4 index values. The diurnal occurrence of scintillation on both bands revealed that it was a completely a night time phenomenon. Scintillation activity commenced at around 20:00 LT reaching a

peak around 23:00 LT and denisnishedbefore 03:00 LT [not sown as Figure].

The five International quiet (Q) and five disturbed (D) days of each month were classified by geomagnetic indices Kp index D-days were noted from the WDC (http://wdc.kugi.kyoto-u.ac.jp/cgi-bin/qddayscgi). The annual average values of VTEC on quiet and disturbed days are shown in Figure 3. The major observation is that the disturbed periods days have higher VTEC values as compared to quiet days VTEC values during the daytime, which is seen almost throughout the year and within seasons (as seen in all panels of Figure 4). The VTEC values tend to be almost the same later in the night time after the hours of 14:00 UT (02:00LT) until almost 21:00UT (0900 LT).

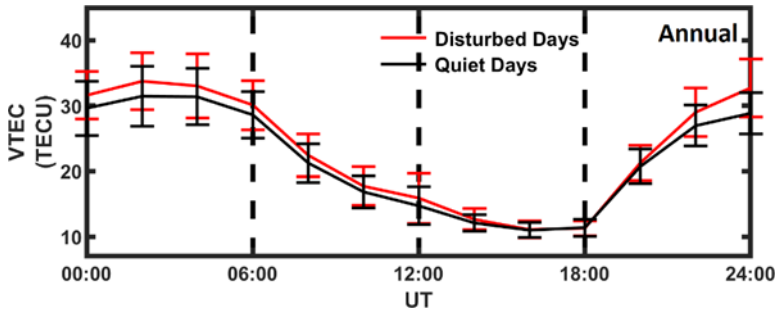

Figure 3. The VTEC variation on geomagnetically quiet and disturbed days at Tarawa from September 2017 to November 2018.

In figure 4, we present geomagnetic (*Dst*, *AE* and *Kp* indices) and solar (X-ray and EUV radiations) activities during 6-9 September 2017, along with VTEC and ΔVTEC% (calculated using Eq. 5). Figure 4a shows the hourly values of the *Dst* and *AE* indices and Figure 4b the three-hourly values of *Kp* index. Figures 4c and d show the variations of solar activity using X-ray (4c) and EUV (4d) radiations, respectively. As seen from Figures 4a & b, the geomagnetic conditions were quiet on 06 September with three hourly *Kp* index within 3 and *Dst* index having mostly positive values. On 6 September, two flares of classes X2.2 at 08:57 UT (20:29 LT) and X9.3 at 11:53 UT (23:25 LT) occurred during the local nighttime of our station, however, M1.4 at 19:21 UT (06:33 LT, 07 Sept) and M1.2 at 23:33UT (11:05 LT, 07 Sept) class flares as indicated in Figure 4c (green font) occurred in the daytime. Figure 4e shows the current TEC variation (solid blue line) during 6-9 September over the mean VTEC (black dashed line) on the five quiet days of the September month. ΔVTEC% calculated using Eq.5 and plotted in Figure 4f shows a variation of about ±10% from the mean value during a period 00-16 UT on 06 September of quiet solar and geomagnetic conditions, which could be considered as natural variability and anything more than 10% we can regard as the TEC perturbations associated with flares and/or geomagnetic storms. On 06 September, associated with X-ray flux and EUV flux (Figure 4d) enhancements of flares M1.4 at 19:21UT (06:53 LT, 07 September) and M1.2 at 23:33 (11:05 LT) class, the VTEC increased from 17:20 UT (04:53 LT) with maximum 16.8% at about 19:05 UT. On 07 September, an M2.4 class flare during the sunlit at 04:59 UT (16:31 LT) and enhanced EUV flux occurred following which VTEC increased sharply with a maximum ΔVTEC% of 30.4%. This VTEC enhancement lasted well into the nighttime.

Following the second interplanetary shock at ~23 UT on 7 September, the first main phase of this storm occurred with a minimum *Dst* value of -142 nT at 01 UT on 8 September as shown in Figure 4a. The *Kp* index increased sharply to a maximum value of 8 at the end of 7 September and the beginning of 8 September producing this G4-class (severe) storm. Then both *Dst* and *Kp* indices recovered gradually until about the end of 8 September. During the first main phase, *AE* index increased to 1157 nT at 23 UT on 07 September. During the first main phase, the VTEC enhanced slightly as seen from ΔVTEC% in Figure 4e. Further contributions to the increase in VTEC came from the daylight side flares of class M3.9 (23:50 UT, 07 September), M1.3 (02:19 UT) and M1.2 (03:39 UT) and sudden bust of EUV radiation as can be seen in Figure 4d, as a result of which ΔVTEC% increased to about 20% at 03:30 UT on 08 September. The VTEC remained enhanced until about 06:30 UT on 8 September following which a negative ionospheric storm occurred with ΔVTEC% of about 22.2% at about 12:15 UT on 08 September which continued well into the second main phase of the storm. The IMF B_Z turned southward sharply at around 11:35 UT on 08 September following which second main phase (or another intense storm) of the storm occurred with a minimum *Dst* value of -124 nT at 17 UT on 8 September. During the recovery phase of the second main phase, VTEC showed a strong long-duration positive ionospheric storm with VTEC sharply increasing with a maximum ΔVTEC% of 32.6% at 03 UT on 09 September. M2.1 class flare at 23:33 UT on 08 September and M1.1 at 04:14 UT on 09 September may have also contributed towards the increase in VTEC. The VTEC increase of more than 10% lasted for a long duration of about 10 hrs (18 UT on 08 September to 04 UT on 09 September). We have selected M3.9 flare to show the VTEC enhancement associated with this flare.

There were also no scintillations observed during the second main phase of this storm, however, later during its recovery phase very weak to weak scintillations occurred at the nighttime from 11:05 – 12:10 UT (22:37 – 23:42 LT) with maximum S_4 index of 0.25 at 11:15 UT (22:47 LT). These amplitude scintillations were associated with stronger σ_ϕ of 0.4 rad and the dTEC of about ±0.8 to 1.0. The *SI* index as had its maximum value of 5.4 dB at 11:15 UT (22:47 LT). Weak to moderate ($0.3 \leq S_4 < 0.45$) scintillations with maximum S_4 index of 0.33 (first event) and 0.35 (second event), *SI* index of about 8 dB (both events) and σ_ϕ of 0.12 rad (first event) and 0.51 rad (second event), occurred on GPS L2 bannd signal [Not shown as Figure].

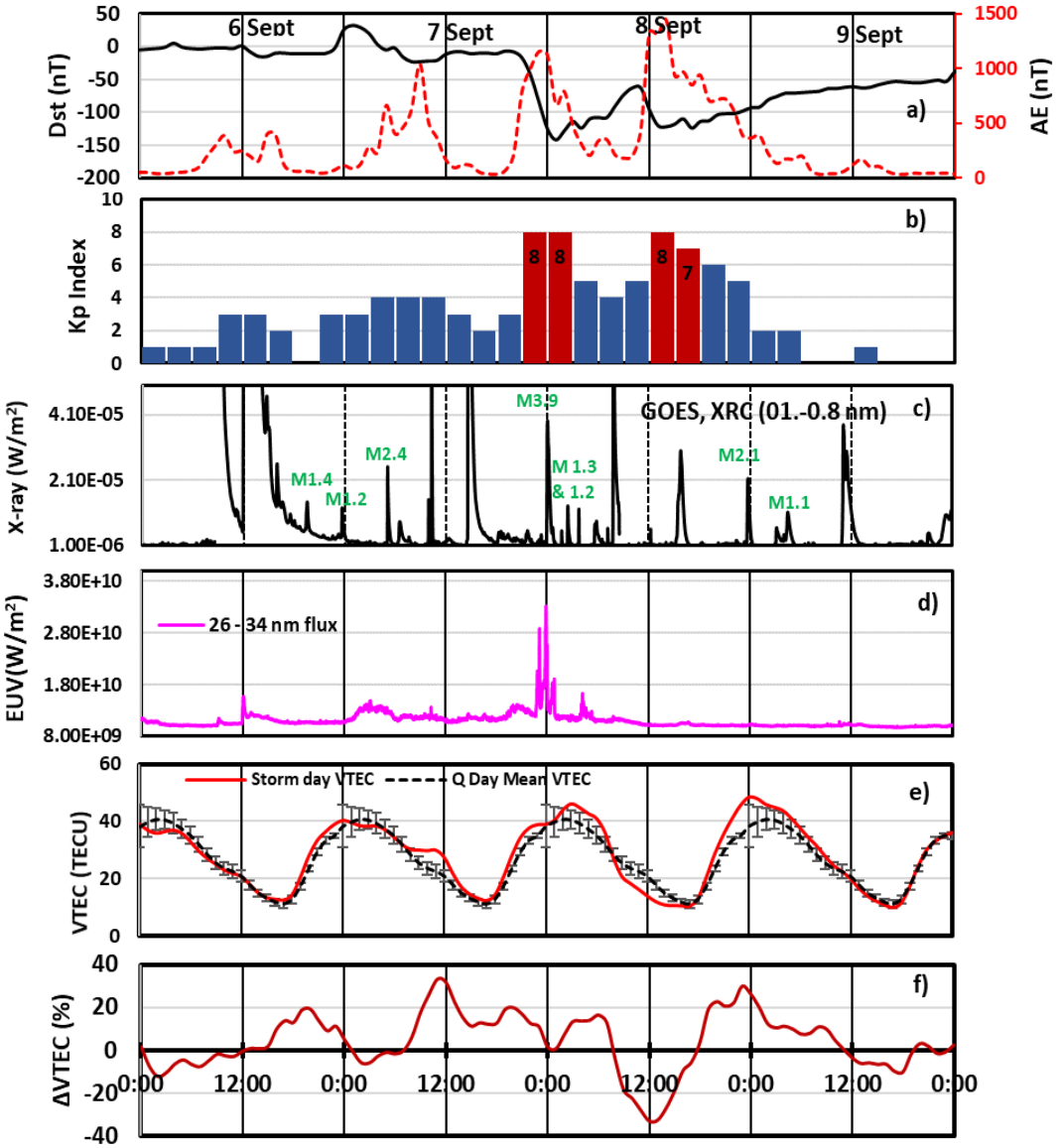

Figure 4. a) Variation of hourly values of *D*st and *AE* indices, b) three hourly *Kp* index, c) X-ray flux recorded by GOES-15XRS (0.1–0.8nm"long"), and d) EUV (26-34 nm) flux. The flares occurring during daytime (18-06 UT) of the receiving station, Tarawa, are indicated in green font, e), the VTEC in TEC units (1TECU = 10^{17}elm^{-3}) and f) changes in storm time VTEC from mean of five geomagnetically most quiet days of September 2017 at the equatorial station, Tarawa, Kiribati, during 6-9 September 2017.

A summary of ionospheric storms at Tamara station due to geomagnetic storms between September 2017 and November 2018 is presented in Table 1. Y stands for yes, indicating the occurrence of positive storm in all phase. The seasons are indicated by E (Equinox), S (Summer) and W (Winter).

Table 1

No.	Min Dst	LT of Step 1	LT of Step 2	Type	Season	Positive Storm/ΔVTEC%	Negative Storm /ΔVTEC%
1	-124	8/9/2017 13:00	9/9/2017 5:00	SSC	E	Y	first step recovery and second main
2	-55	28/9/2017 18:00		SGC	E	Y	-
3	-74	7/11/2017 19:00	8/11/2017 13:00	SGC	W	Y	first step main and recovery
4	-66	20/4/2018 21:00	21/4/2018 6:00	SSC	E	Y	-
5	-56	6/5/2018 6:00	6/5/2018 14:00	SSC	S	Y	-
6	-174	26/8/2018 19:00		SGC	S	Y	2-4 recovery days
7	-60	11/9/2018 11:00	11/9/2018 22:00	SGC	E	Y	-

The geomagnetic storms generated both positive and negative ionospheric storms. The positive ionospheric effects dominantly occurred during the main phase of all the storms which can be attributed to the prompt penetration plectric field (PPEF). Negative ionospheric storm effects were observed during the recovery phase of the storms and were a night time phenomenon. These can be accounted for disturbance dynamo electric field (DDEF) and storm-induced circulation of high latitude gas with depleted O/N_2 density ratio. The PPEF and DDEF can couple the high and low latitude ionosphere and thermosphere causing changes in the ambient electric field at the equator. PPEF is generated promptly when IMF persists for 30-120 min and occurs due to the difference in the north and south polar cap potential caused by the interaction of the solar wind with the magnetosphere under the southward B_Z condition. The changes in the storm time electric field (or PPEF) can cause changes in the **E×B** drift by uplifting the F region plasma and redistributing it in the EIA crests according to the strength of PPEF.

The effects of Space weather phenomena (geomagnetic storms and solar flares) on the equatorial and low latitude ionosphere studied in project indicate that ionospheric electron content is significantly changed (increase/decrease) particularly under intense geomagnetic storms that can cause significant errors on global navigation satellite system (GNSS) based navigation services. The spaceborne measurements of positioning, displacements, navigation, and timing play an important and critical role in telecommunications, all forms of transportation, and other human activities. A further study on the ionospheric effects and resultant GNSS signal delays due to a large no of space weather events on equatorial and low latitude ionosphere is recommended to quantify the ionosphere delay for the GNSS under varying space weather conditions.

List of Publications and Significant Collaborations that resulted from your AOARD supported project: In standard format showing authors, title, journal, issue, pages, and date, for each category list the following:

a) papers published in peer-reviewed journals,

1. Kumar, S., & Kumar, V. V. (2019).Ionospheric response to the St. Patrick's Day space weather events in March 2012, 2013, and 2015 at southern low and middle latitudes. Journal of Geophysical Research: Space Physics, 124. https://doi.org/10.1029/2018JA025674.

b) papers published in peer-reviewed conference proceedings,
No

c) papers published in non-peer-reviewed journals and conference proceedings,

d) No

e) conference presentations without papers,

1. Sarvesh Kumar and **Sushil Kumar**, Total Electron Content at an Equatorial Station: Space Weather Control, Accepted for Presentation in "43rd COAPAR Scientific Assembly (COSPAR 2021), 28 January- 4 February 2021, Sydney, Australia.
2. **Sushil Kumar** and Sarvesh Kumar, Equatorial Ionospheric Response to the Space Weather Events of 4-10 September 2017, Poster presentation at 2019 AGU Fall Meeting, San Francisco, California, USA, 09-13 December 2019.
3. **Sushil Kumar**, Ionospheric response to Space Weather Events in March 2013 and 2015 and Comparison with Similar Strength Storms of July 2012 and June 2015, Presented (oral) to Workshop Applications of Global Navigation Satellite Systems (GNSS), The University of the South Pacific, Suva, 24-28 June 2019.
4. **Sushil Kumar**, Ionospheric Response to Space Weather Events in the South Pacific Region, Presented (oral) in 4th AOARD Australian and New Zealand Workshop on Space Situation Awareness 2018, University of New South Wales, Canberra, Australia, 25-27 July 2018
5. **Sushil Kumar**, F-2 Region Response to the Storms Near St. Patrick's Day in March 2013 and 2015 at the Low and Mid Latitude Stations in the Southern Hemisphere, Presented in 15th AOGS Annual Meeting/conference, 03-08 June, 2018, Honululu, Hawaii, USA.

f) manuscripts submitted but not yet published, and

1. Manuscript Number: JASTP-D-20-00023, Equatorial Ionospheric TEC and Scintillations under the Space Weather Events of 4-9 September 2017: M-Class Solar Flares and a G4 Geomagnetic Storm, Communicated for publication in Journal of Solar-Atmospheric Physics on 23rd February 2020 and paper is under revision after review.

g) provide a list any interactions with industry or with Air Force Research Laboratory scientists or significant collaborations that resulted from this work.

1. During AGU 2019, a lunch meeting was held with Dr. L. C. Gentile and her two colleagues from Air Force Research Laboratory (AFRL), 12 December with the main discussion on installing atmospheric equatorial radar at the Kiribati Campus of The University of the South Pacific (USP) under our project funded by AFRL.
2. A new Global Navigation Satellite Systems (GNSS) station for Ionospheric Monitoring and Precise Point Positioning (PPP) Research was installed in December 2019 in Physics under an MoU between School of Engineering and Physics (SEP), The University of the South Pacific (USP) and the School of Electronics and Information Engineering (SEIE), Beihang University, China.

JGR Space Physics

RESEARCH ARTICLE
10.1029/2018JA025674

Ionospheric Response to the St. Patrick's Day Space Weather Events in March 2012, 2013, and 2015 at Southern Low and Middle Latitudes

Sushil Kumar[1] and Vickal V. Kumar[2]

[1]School of Engineering and Physics, The University of the South Pacific, Suva, Fiji, [2]Space Weather Services, Australian Bureau of Meteorology, New South Wales, Australia

Key Points:

- A strong long-duration decrease in f_oF_2 was found during the recovery phase of the St. Patrick's Day storms in March 2012, 2013 and 2015
- A short-duration strong increase in f_oF_2 occurred during the recovery phase of similar strength June 2015 storm in contrast to the March 2015 storm
- The decrease in f_oF_2 given by the IRI-2016 model is smooth but less than that shown by ionosonde data for both the March 2013 and 2015 storms

Correspondence to:
S. Kumar,
skumar6873@gmail.com

Citation:
Kumar, S., & Kumar, V. V. (2019). Ionospheric response to the St. Patrick's Day space weather events in March 2012, 2013, and 2015 at southern low and middle latitudes. *Journal of Geophysical Research: Space Physics, 124*. https://doi.org/10.1029/2018JA025674

Abstract The changes in critical frequency of the F_2 layer (f_oF_2) and f_oF_2 deviation (Δf_oF_2) have been determined for three geomagnetic storms in March of the years 2012, 2013, and 2015 at low-latitude stations, Darwin (geomag. lat. 21.96°S) and Townsville (28.95°S), and midlatitude stations, Brisbane (36.73°S), Canberra (45.65°S), and Hobart (54.17°S). The moderate storm during 15–16 March 2012 (Dst = −87 nT) showed a decrease in f_oF_2 at midlatitude and no effect at low-latitude stations. For the intense storm of 17–18 March 2013 (Dst = −132 nT) and the super storm of 17–18 March 2015 (Dst = −222 nT), some middle- to low-latitude stations showed a short-duration increase in f_oF_2, but all stations showed a long-duration decrease in f_oF_2 during the recovery phases with Δf_oF_2% varying from 26% (Darwin) to 36.6% at Hobart for the March 2013 storm and above 40% for the March 2015 storm at all of the stations. Short-duration (~2–4 hr) increase in f_oF_2 seems to be associated with the prompt penetrating electric fields. Long-duration (>6 hr) decrease in f_oF_2 is mainly accounted to the decrease in thermospheric O/N_2 density ratio because of storm-induced high-latitude circulation of gas with depleted O/N_2 density ratio to lower latitudes and partly due to disturbance dynamo electric fields. A comparison of ionosonde given f_oF_2 for equinoctial storms (March 2013 and 2015) with similar strength Southern Hemisphere winter storms (July 2012 and June 2015) has been made with the IRI-2016 model f_oF_2 for Darwin, Brisbane, and Canberra stations.

Acknowledgments
Author (S. K.) is thankful to the Asian Office of Aerospace Research and Development (AOARD), Japan, for the funding award FA2386-17-1-0054, under this work, has been carried out. The f_oF_2 data were obtained from the World Data Centre, Bureau of Meteorology, Australia (online at http://www.sws.bom.gov.au/World_Data_Centre). The *Dst* and *AE* indices values were obtained from the World Data Centre, Kyoto University, Kyoto, Japan (online at http://www.ssde.u-kigi-kyoto-ac.jp). The IRI 2016 model was run online at https://omniweb.gsfc.nasa.gov/vitmo/IRI-2016_vitmo.html. The IMF B_Z plots recorded by ACE magnetometer data were obtained from ACE Science Center through http://www.srl.caltech.edu/ACE/ASC/level2/index.html. The thermospheric O/N2 density data from the GUVI were obtained from the web resource of John Hopkins University Applied Physics Laboratory (http://guvitimed.jhuapl.edu).